The American Journal of Pathology, Vol. 185, No. 5, May 2015

ELSEVIER

The American Journal of PATHOLOGY

ajp.amjpathol.org

METABOLIC, ENDOCRINE, AND GENITOURINARY PATHOBIOLOGY

PPARα-Deficient *ob/ob* Obese Mice Become More Obese and Manifest Severe Hepatic Steatosis Due to Decreased Fatty Acid Oxidation

Qian Gao,*† Yuzhi Jia,* Gongshe Yang,† Xiaohong Zhang,* Prajwal C. Boddu,* Bryon Petersen,‡ Saiprasad Narsingam,* Yi-Jun Zhu,* Bayar Thimmapaya,§ Yashpal S. Kanwar,* and Janardan K. Reddy*

From the Departments of Pathology and Microbiology and Immunology,§ Feinberg School of Medicine, Northwestern University, Chicago, Illinois; the Laboratory of Animal Fat Deposition and Muscle Development,† College of Animal Science and Technology, Northwest A&F University, Shaanxi, China; and the Department of Pediatrics,‡ Child Health Research Institute, College of Medicine, University of Florida, Gainesville, Florida*

Accepted for publication January 12, 2015.

Address correspondence to Janardan K. Reddy, M.D., Department of Pathology, Feinberg School of Medicine, Northwestern University, 303 E Chicago Ave, Chicago, IL 60611. E-mail: jkreddy@northwestern.edu.

Obesity poses an increased risk of developing metabolic syndrome and closely associated nonalcoholic fatty liver disease, including liver cancer. Satiety hormone leptin-deficient (*ob/ob*) mice, considered paradigmatic of nutritional obesity, develop hepatic steatosis but are less prone to developing liver tumors. Sustained activation of peroxisome proliferator–activated receptor α (PPARα) in *ob/ob* mouse liver increases fatty acid oxidation (FAO), which contributes to attenuation of obesity but enhances liver cancer risk. To further evaluate the role of PPARα-regulated hepatic FAO and energy burning in the progression of fatty liver disease, we generated PPARα-deficient *ob/ob* (PPARα$^{\Delta}$*ob/ob*) mice. These mice become strikingly more obese compared to *ob/ob* littermates, with increased white and brown adipose tissue content and severe hepatic steatosis. Hepatic steatosis becomes more severe in fasted PPARα$^{\Delta}$*ob/ob* mice as they fail to up-regulate FAO systems. PPARα$^{\Delta}$*ob/ob* mice also do not respond to peroxisome proliferative and mitogenic effects of PPARα agonist Wy-14,643. Although PPARα$^{\Delta}$*ob/ob* mice are severely obese, there was no significant increase in liver tumor incidence, even when maintained on a diet containing Wy-14,643. We conclude that sustained PPARα activation–related increase in FAO in fatty livers of obese *ob/ob* mice increases liver cancer risk, whereas deletion of PPARα in *ob/ob* mice aggravates obesity and hepatic steatosis. However, it does not lead to liver tumor development because of reduction in FAO and energy burning. *(Am J Pathol 2015, 185: 1396–1408; http://dx.doi.org/10.1016/j.ajpath.2015.01.018)*

Obesity, a disorder involving chronic energy imbalance resulting from excess caloric intake and reduced energy expenditure, was estimated to affect 671 million adults globally in 2013.[1,2] Furthermore, in 2013, another 1.4 billion adults were considered to become overweight.[1] Overall, the prevalence of overweight with a body mass index of $\geq$25 to <30 kg/m^2, and obesity with a body mass index of $\geq$30 kg/m^2, in adults aged >18 years has increased substantially during the past three decades (1980 to 2013).[1] In the United States, obesity rates are among the highest in the world, with approximately 70% of Americans being overweight or obese.[2] Because of the established health risks, such as insulin resistance, metabolic syndrome, type 2 diabetes mellitus, atherogenic dyslipidemia, and nonalcoholic fatty liver disease, obesity has become a major global health challenge.[1] Nonalcoholic fatty liver disease of obesity begins with simple hepatic steatosis that progresses to nonalcoholic steatohepatitis with inflammation, hepatocellular injury, liver cell proliferation, and fibrous scarring, culminating in end-stage liver disease of cirrhosis and liver cancer.[3–6] On the basis of the burgeoning pandemic of nutritional obesity, it is projected that 25 million Americans will likely develop nonalcoholic

Supported by NIH grants DK083163 and DK097240 (J.K.R.), R21A1094296 (B.T.), DK60015 and DK58614 (B.P.), and DK60635 (Y.S.K.) and the China Scholarship Council grant CSC 2011630169 (Q.G.).

The funders had no role in the study design, data collection and analysis, decision to publish, or preparation of the manuscript.

Disclosures: None declared.

http://dx.doi.org/10.1016/j.ajpath.2015.01.018

steatohepatitis by 2025, with approximately 20% progressing to cirrhosis of liver, with an added risk of developing hepatocellular carcinoma.[7]

In obesity, the unburnt energy is conserved in the form of fat (triacylglycerol), first in adipocytes considered limitless reservoirs of fat and subsequently in liver considered as a surrogate reservoir for fat, when adipose fat stores are nearly saturated.[8–10] Liver is a central player in whole body energy homoeostasis by its ability to metabolize glucose and fatty acids, with surplus glucose converted to fat for storage.[11] Hepatic steatosis occurs under a variety of conditions, especially when the rate of hepatic fatty acid uptake from plasma and *de novo* fatty acid synthesis from glucose is greater than the rate of fatty acid oxidation (FAO).[12] Excess storage of lipid in liver without inflammation (bland hepatic steatosis) by itself is insufficient to increase liver cancer risk in obesity, as noted in *ob/ob* mice deficient in satiety hormone leptin.[13] Enhancement of FAO in these *ob/ob* fatty livers by sustained activation of peroxisome proliferator–activated receptor (PPAR)-α leads to nonalcoholic steatohepatitis and enhanced endoplasmic reticulum stress, contributing to a high incidence of liver tumors.[14] PPARα, because of its unique ability to regulate FAO in liver, plays a significant role in the pathogenesis of hepatic steatosis and in the development of hepatocellular carcinomas in rats and mice.[15,16] PPARα-null mice (*PPARα*$^{-/-}$) are unable to up-regulate the expression of FAO-associated genes and, as a consequence, they develop hepatic steatosis but fail to develop liver tumors in response to chronic exposure to peroxisome proliferators.[17–19] Accordingly, these observations support the concept that PPARα-regulated increases in FAO contribute to the development of liver tumors in nonalcoholic fatty liver disease.[3,4]

Herein, we examined the impact of PPARα deficiency on the obesity and fatty liver of leptin-deficient mice. PPARα-deficient mice were crossed with heterozygous leptin-deficient *OB/ob* mice to generate PPARα-deficient *ob/ob* (PPARα$^{\Delta}$*ob/ob*) mice. Deletion of PPARα in these obese *ob/ob* mice aggravates obesity because of increases in white and brown fat content and fasting-induced hepatic steatosis because of the failure to increase fatty acid oxidation capacity in the absence of PPARα. Despite severe hepatic steatosis, PPARα$^{\Delta}$*ob/ob* mice do not develop liver tumors, because they fail to increase FAO and energy burning necessary for the induction of oxidative and endoplasmic reticulum stresses that play a role in liver tumor development.[14,15]

Materials and Methods

Animals

Acox1-deficient (*Acox1*$^{-/-}$) mice[20] and PPARα-deficient (PPARα$^{-/-}$) mice[21] were maintained on a C57BL/6J background as breeding colonies. The generation of *Acox1*-deficient *ob/ob* (Acox1$^{\Delta}$*ob/ob*) mice was described previously.[22] To generate PPARα-deficient *ob/ob* mice (PPARα$^{\Delta}$*ob/ob*), heterozygous leptin-deficient *OB/ob* mice (The Jackson Laboratory, Bar Harbor, ME) were crossed with PPARα$^{-/-}$ mice to obtain heterozygous PPARα$^{+/-}$/*OB/ob* mice, which were further bred to produce PPARα-deficient *ob/ob* double-mutant mice designated PPARα$^{\Delta}$*ob/ob* mice (Supplemental Figure S1).

The mice were genotyped by PCR of genomic DNA isolated from tail tips obtained at the age of 3 weeks. To identify *ob/ob* mice, primers used were as follows: 5′-TGTCCAAGATGGACCAGACTC-3′ (forward) and 5′-ACTGGTCTGAGGCAGGGAGCA-3′ (reverse). For PPARα-null mice, the primers used were as follows: 5′-CTTGGGTGGAGAGGCTATTC-3′ (forward) and 5′-AGGTGAGATGACAGGAGATC-3′ (reverse). For genotyping *Acox1* mice, the primers used were as follows: 5′-TATTCGGCTATGACTGGGCACA-3′ (forward) and 5′-GATGGATACTTTCTCGGCAGGA-3′ (reverse).[22]

All mice were maintained in polypropylene cages in a temperature-controlled (23°C) environment using a standard photoperiod (12 hours light and 12 hours dark cycle) with lights on at 6 AM. Mice were provided rodent chow (Teklad 7904; Harlan-Teklad, Indianapolis, IN) with or without added PPARα activator Wy-14,643 (0.05% or 0.125% w/w) and water ad libitum.

For food intake measurement, three mice were housed individually, and the daily caloric intake was determined over a 7-day period and normalized against the initial body weight (kcal/g body weight per day). These measurements were repeated three times using different batches of mice. To assess hepatocyte proliferation, mice were administered 0.5 mg/mL bromodeoxyuridine (BrdUrd) in drinking water and sacrificed at the end of 3 days. All procedures of animal handling were approved by the Institutional Animal Care and Use Committees of Northwestern University (Chicago, IL; protocol number 2013-3198).

Glucose Tolerance and Insulin Tolerance Tests

Wild-type (WT), PPARα$^{-/-}$, *ob/ob*, and PPARα$^{\Delta}$*ob/ob* mice (aged 3 months; five mice in each group) were used for determining glucose tolerance and insulin tolerance essentially as described previously.[22] Briefly, glucose (1.5 mg/g body weight in phosphate-buffered saline) was administered i.p. to mice that were maintained without food for 6 hours.[22,23] Blood obtained from tail vein at 0, 30, 60, and 120 minutes after administering glucose was used for measuring glucose using a glucose meter (One Touch; LifeScan, Milpitas, CA). For testing insulin tolerance, mice deprived of food for 4 hours were given insulin (0.75 mU/g body weight in phosphate-buffered saline; Sigma, St. Louis, MO) by an i.p. injection. Blood glucose levels were determined at 0, 15, 30, and 60 minutes after insulin injection.

Table 1 Primers for Genotyping, Quantitative PCR, and Northern Blot Analysis

Primer name	Forward primer	Reverse primer
PPARα ko geno	5′-CTTGGGTGGAGAGGCTATTC-3′	5′-AGGTGAGATGACAGGAGATC-3′
PPARα wt geno	5′-CCATCCAGATGACACCTTCC-3′	5′-TCTCTTGCAACAGTGGGTGC-3′
ob/ob geno	5′-TGTCCAAGATGGACCAGACTC-3′	5′-ACTGGTCTGAGGCAGGGAGCA-3′
Neo geno	5′-TATTCGGCTATGACTGGGCACA-3′	5′-GATGGATACTTTCTCGGCAGGA-3′
ACOX1 geno	5′-CCGCAAGCCATCCGACATTC-3′	5′-ATTCAGTGGGTCAGGCGACTGC-3′
PPARα	5′-GGGCTCCGAGGGCTCTGTCA-3′	5′-TGCAGCTCCGATCACACTTGTCG-3′
Acox1	5′-GCCAAGGCGACCTGAGTGAGC-3′	5′-ACCGCAAGCCATCCGACATTC-3′
L-PBE/*Ehhadh*	5′-GGTCGTTGGAGTTCCTGTTGCT-3′	5′-TGGGCAAGCTTGGGACTGGC-3′
SCAD	5′-GCTGAGTGGTGCAGGCTTG-3′	5′-CCATTGGTGAAAGGGGTGATC-3′
MCAD	5′-GGATGACGGAGCCAATG-3′	5′-GGGTGTCGGCTTCCACAATG-3′
LCAD	5′-GACGGCGGGCAAGTGTATC-3′	5′-GCAGGCGATCGAGCTTCAC-3′
Cyp4a1	5′-AGGATGAGGGAGAGCTGGAAAAGAT-3′	5′-GACTCCACTGGCTGTGGTGTCATG-3′
Cyp4a3	5′-GCAGAAGGCCAGGAAGAGACAC-3′	5′-CCAGAGCATAGAAAATCCAGGAAATT-3′
PPARγ	5′-CCACAGTTGATTTCTCCAGCATTTC-3′	5′-CAGGTTCTACTTTGATCGCACTTTG-3′
PGC1α	5′-CTCCATGCCTGACGGCACCC-3′	5′-GCAGGGACGTCTTTGTGGCT-3′
Sirt1	5′-GGATGATATGACGCTGTGGC-3′	5′-AGAGACGGCTGGAACTGTCC-3′
FGF21	5′-TGGGGGTCTACCAAGCATAC-3′	5′-AAGGCTCTACCATGCTCAGG-3′
PEPCK	5′-TGAACTGACAGACTCGCCCT-3′	5′-GTCTTCCCACAGGCACTAGG-3′
PTL	5′-TCTCCAGGACGTGAGGCTAAA-3′	5′-CGCTCAGAAATTGGGCGATG-3′
Nrf2	5′-GATGGACTTGGAGTTGCCAC-3′	5′-GTTTGGGAATGTGGGCAACC-3′
P8	5′-CTCCCTCTCCAGAACCTCACT-3′	5′-ACCAAGAGAGAAGCTGCTGC-3′
18S	5′-AAACGGCTACCACATCCAAG-3′	5′-CCTCCAATGGATCCTCGTTA-3′

ACOX, acyl-Coenzyme A oxidase; FGF, fibroblast growth factor; LCAD, long-chain acyl-CoA dehydrogenase; L-PBE, L-3-hydroxyacyl-CoA dehydrogenase; MCAD, medium-chain acyl-CoA dehydrogenase; PEPCK, phosphoenolpyruvate carboxykinase; PGC, peroxisome proliferator-activated receptor gamma, coactivator; PPAR, peroxisome proliferator—activated receptor; PTL, 3-ketoacyl-CoA thiolase; SCAD, short-chain acyl-CoA dehydrogenase.

Biochemical Assays

Liver samples were homogenized for extraction of lipid using chloroform/methanol method. Triacylglycerol (Thermo Electron, Louisville, CO) and total cholesterol (Wako Diagnostics, Richmond, VA) levels were determined as described elsewhere.[24] Blood obtained from retro-orbital veins was used for triglyceride and total cholesterol determinations.[25,26]

Histology and Immunohistochemistry

For histological analysis, liver slices were fixed in 4% paraformaldehyde and processed for embedding in paraffin. Paraffin sections (4 μm thick) were cut and stained with hematoxylin and eosin. For visualization of cellular fat, frozen sections of liver (approximately 5 μm thick) were stained with 0.5% Oil Red O solution for 30 minutes in a 60°C oven and then in 85% propylene glycol solution for 5 minutes. After rinsing with distilled water, sections were stained with Gill's hematoxylin for 2 seconds, washed, and mounted with aqueous mounting medium.[22,27] Paraffin sections were also used for Sirius Red staining.[28] Liver sections were also processed for the localization of catalase, L-PBE (enoyl-Coenzyme A, hydratase; *EHHADH*), and BrdUrd, as described elsewhere.[20,29] BrdUrd nuclear labeling indices were obtained by analyzing immunohistochemically stained liver sections.[30] All images were acquired by a light microscope adapted to a high-resolution camera (AxioCam; Carl Zeiss, Oberkochen, Germany) and analyzed by the computer using AxioVisionRel software version 4.8 (Carl Zeiss).

Immunoblotting

For immunoblotting, 40 μg liver protein samples were subjected to 4% to 20% SDS-PAGE, transferred to nitrocellulose membrane, and blotted using antibodies against PPARα, L-3-hydroxyacyl-CoA dehydrogenase (L-PBE), acyl-CoA oxidase 1, palmitoyl (Acox1), short-chain acyl-CoA dehydrogenase (SCAD), medium-chain acyl-CoA dehydrogenase (MCAD), long-chain acyl-CoA dehydrogenase, peroxisomal 3-ketoacyl-CoA thiolase A (PTL), D-3-hydroxyacyl-CoA dehydratase (D-PBE), and catalase, as described elsewhere.[29,31] β-Actin (antibody sc-47778; Santa Cruz Biotechnology, Inc., Santa Cruz, CA) was used as loading control.

Northern Blotting and Real-Time PCR

Total RNA was isolated from mouse liver with TRIzol reagent (Invitrogen, Life Technologies, Carlsbad, CA). For Northern blotting, RNA was glyoxylated, separated on a 1% agarose gel, transferred to a nylon membrane, hybridized at 65°C in Rapid-hyb buffer (GE Healthcare, Piscataway, NJ), and probed with α-^{32}P—labeled cDNA.[29,32] RNAs (28S and 18S) were set as the loading controls. For real-time PCR, total RNA isolated from liver was reverse transcribed to make cDNA using the Superscript III first-strand synthesis system for RT-PCR (Invitrogen Life Technologies). The primers used for the real-time PCR are listed in Table 1. Quantitative expression of genes was checked using SYBR Green (Applied Biosystems, Foster City, CA) in triplicate and normalized with 18S ribosomal RNA. PCR was composed of 1 μL (100 ρmol)

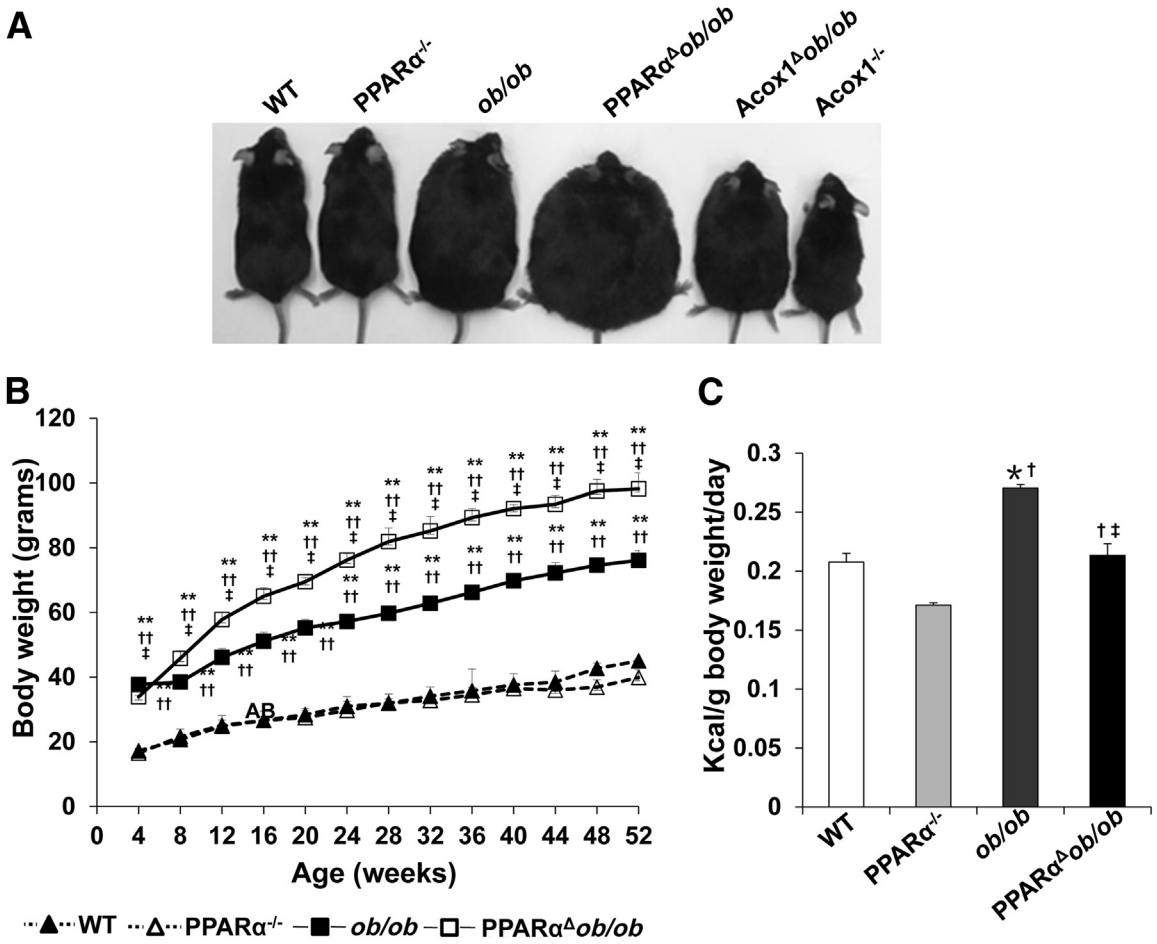

Figure 1 PPARα$^{\Delta}$*ob/ob* mice become super obese. **A:** Physical appearance of chow-fed 16-month-old wild-type (WT), PPARα$^{-/-}$, *ob/ob*, and PPARα$^{\Delta}$*ob/ob* mice. Acox1$^{\Delta}$*ob/ob* and *Acox1*$^{-/-}$ mice that manifest PPARα activation by endogenous ligands are included for comparison. **B:** Age-related body weight changes of WT, PPARα$^{-/-}$, *ob/ob*, and PPARα$^{\Delta}$*ob/ob* mice, aged 4 to 52 weeks. **C:** For food consumption estimation, three mice in each group were housed in separate cages, and daily food intake (kcal) per body weight was determined by measuring 7-day consumption. *$P < 0.05$, **$P < 0.01$ versus WT; $^{\dagger}P < 0.05$, $^{\dagger\dagger}P < 0.01$ versus PPARα$^{-/-}$; $^{\ddagger}P < 0.05$ versus *ob/ob*.

of forward and reverse primers and 10 μL of 2× SYBR Green PCR Master Mix and performed by using an ABI 7300 system (Applied Biosystems). The generation of specific PCR products was confirmed by melting curve analysis, and the relative gene expression changes were measured using the comparative Ct method: $X = 2^{-\Delta\Delta Ct}$.

Statistical Analysis

Data were analyzed by one-way analysis of variance using SPSS software version 11.5 (SPSS, Chicago, IL). $P < 0.05$ was considered significant.

Results

Obese *ob/ob* Mice Lacking PPARα Become Super Obese

Because of subfertility of homozygous *ob/ob* mice, heterozygous *OB/ob* mice were mated with PPARα$^{-/-}$ (PPARα$^{-/-}$ with *OB/OB*) mice to generate double-heterozygous PPARα$^{+/-}$ *OB/ob* mice. These mice, when intercrossed, yielded PPARα$^{\Delta}$*ob/ob* mice used in these studies (Supplemental Figure S1A). PCR amplification of genomic DNA from double-nullizygous PPARα$^{\Delta}$*ob/ob* mice yielded 55- and 100-bp bands for *ob/ob* and a 280-bp band for PPARα$^{-/-}$ (Supplemental Figure S1B). DNA from WT mice showed one 143-bp band and one 155-bp band for PPARα$^{+/+}$ and *OB/OB*, separately (Supplemental Figure S1B).

PPARα mediates the pleiotropic responses induced in liver by peroxisome proliferators.[16,21,33] These include hepatomegaly, peroxisome proliferation, and transcriptional activation of genes encoding peroxisomal, mitochondrial, and microsomal FAO enzymes.[16,34] Previous studies demonstrated that *Acox1* deletion disrupts metabolism in WT mice, and *ob/ob* mice are smaller and leaner than both WT and *ob/ob* mice.[20,22] In the absence of *Acox1*, the unmetabolized substrates of this enzyme serve as endogenous PPARα activators.[16,32] Sustained activation of PPARα by its endogenous ligands in Acox1$^{\Delta}$*ob/ob* mice (Figure 1A) increases hepatic fatty acid oxidation and attenuates obesity.[22] In contrast,

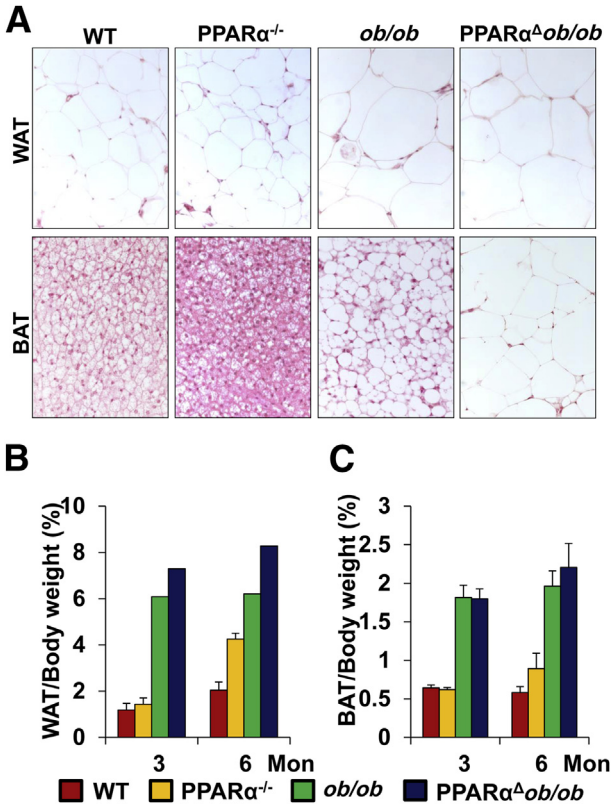

Figure 2 Fat accumulation in the inguinal white adipose tissue (WAT) and scapular brown adipose tissue (BAT). **A:** Histological features of WAT and BAT of 3-month-old wild-type (WT), PPARα$^{-/-}$, *ob/ob*, and PPARα$^{\Delta}$*ob/ob* mice. **B** and **C:** Fat:body weight ratios.

deletion of PPARα in the *ob/ob* background (PPARα$^{\Delta}$*ob/ob*) resulted in a further increase in somatic growth compared to their *ob/ob* littermates (Figure 1, A and B). From weaning until approximately the age of 6 weeks, somatic growth of PPARα$^{\Delta}$*ob/ob* mice did not significantly differ from *ob/ob* mice. However, by the age of 24 weeks, PPARα$^{\Delta}$*ob/ob* mice gained more weight than *ob/ob* mice and were distinctly more obese (super obese) than *ob/ob* mice (Figure 1, A and B). There was no significant difference in food intake of WT and PPARα$^{-/-}$ mice, but food consumption in *ob/ob* mice was slightly more than that of PPARα$^{\Delta}$*ob/ob* mice. These findings suggest that increased obesity observed in PPARα$^{\Delta}$*ob/ob* mice is not due to increased food intake but related to decreased energy expenditure associated with PPARα deletion (Figure 1C).

Examination of 3- and 6-month-old PPARα$^{\Delta}$*ob/ob* and *ob/ob* mice revealed a consistent increase in the amount of inguinal white adipose tissue (WAT) and interscapular brown adipose tissue (BAT) in both *ob/ob* and PPARα$^{\Delta}$*ob/ob* mice, but the increase was more prominent in double nulls (Supplemental Table S1). At 6 months of age, the WAT in WT mice was 0.56 g compared to 4.22 g in *ob/ob* mice and 5.87 g in PPARα$^{\Delta}$*ob/ob* mice. In 6-month-old WT mouse, BAT was 0.14 g compared to 1.19 g in *ob/ob* mice and 1.37 g in PPARα$^{\Delta}$*ob/ob* mice (Supplemental Table S1).

Histological examination of WAT revealed no significant difference in the adipocyte size of PPARα$^{\Delta}$*ob/ob* mice when compared with *ob/ob* mice (Figure 2A). In both *ob/ob* and *PPARα*$^{\Delta}$*ob/ob* mice, BAT whitened with several large lipid droplets, and this change was considerably greater in PPARα$^{\Delta}$*ob/ob* mice (Figure 2A). At 6 months of age, the WAT and BAT body weight ratios were increased in PPARα$^{\Delta}$*ob/ob* mice (Figure 2, B and C). Leptin-deficient *ob/ob* mice exhibit hyperphagia and obesity, along with hyperglycemia and hyperinsulinemia.[35] PPARα knockout mice appear normal, but the circulating glucose is lower, with increased serum insulin level.[23] PPARα$^{\Delta}$*ob/ob* mice exhibited higher serum glucose level and lower insulin level compared with WT and *ob/ob* mice (Supplemental Figure S2, A and B). PPARα deficiency improved insulin and glucose tolerance in obese mice.

PPARα Deficiency Aggravates Hepatic Steatosis in *ob/ob* Mice

PPARα deficiency in *ob/ob* mice results in an increased accumulation of fat in liver as compared to that in *ob/ob* livers (Figure 3). At 3 and 6 months of age, liver/body weight ratios were higher in PPARα$^{\Delta}$*ob/ob* mice than in *ob/ob* mice (Supplemental Table S1), and on histological examination, including Oil Red O staining for fat, these livers revealed prominent macrovesicular steatosis (Figure 3). Overall, in PPARα$^{\Delta}$*ob/ob* mouse hepatocytes, fat droplets appeared much larger at 3 and 6 months of age (Figure 3). Hepatic triglyceride and cholesterol content was higher in 6-month-old PPARα$^{\Delta}$*ob/ob* mice as compared to WT, PPARα$^{-/-}$, and *ob/ob* mice (Supplemental Figure S2, C and D).

Aging Attenuates Hepatic Steatosis in PPARα$^{\Delta}$*ob/ob* Mice and Induces Hepatic Oval Cell Proliferation

There was a reduction in hepatic steatosis in both *ob/ob* and PPARα$^{\Delta}$*ob/ob* mice aged 16 months or older (Figure 3). In PPARα$^{\Delta}$*ob/ob* mice, liver displayed cellular heterogeneity with mild pericellular fibrosis and emerging clusters of oval cells (Figure 3). Severe hepatic steatosis in double-knockout mice increased hepatocyte apoptosis and hepatocyte regeneration independent of *PPARα* to replace the dead liver cells (data not shown). Oval cells in PPARα$^{\Delta}$*ob/ob* mouse liver, occurring either singly or in clusters, stained positively on immunohistochemical analysis (Supplemental Figure S3A) for oval cell markers A6, CD45, CK19, and epithelial cell adhesion molecule.[36,37] Quantitative PCR analysis revealed robust expression of these genes in aged PPARα$^{\Delta}$*ob/ob* mouse livers, but albumin levels were low and α-fetoprotein was high (Supplemental Figure S3B).

Severe Fatty Liver in Fasted PPARα$^{\Delta}$*ob/ob* Mice

During periods of starvation, triglycerides stored in adipose tissue are hydrolyzed to free fatty acids and mobilized into plasma to reach liver. In liver, they are oxidized by the mitochondrial β-oxidation system and, to a lesser extent, by the peroxisomal β-oxidation, as well as by CYP4A-catalyzed

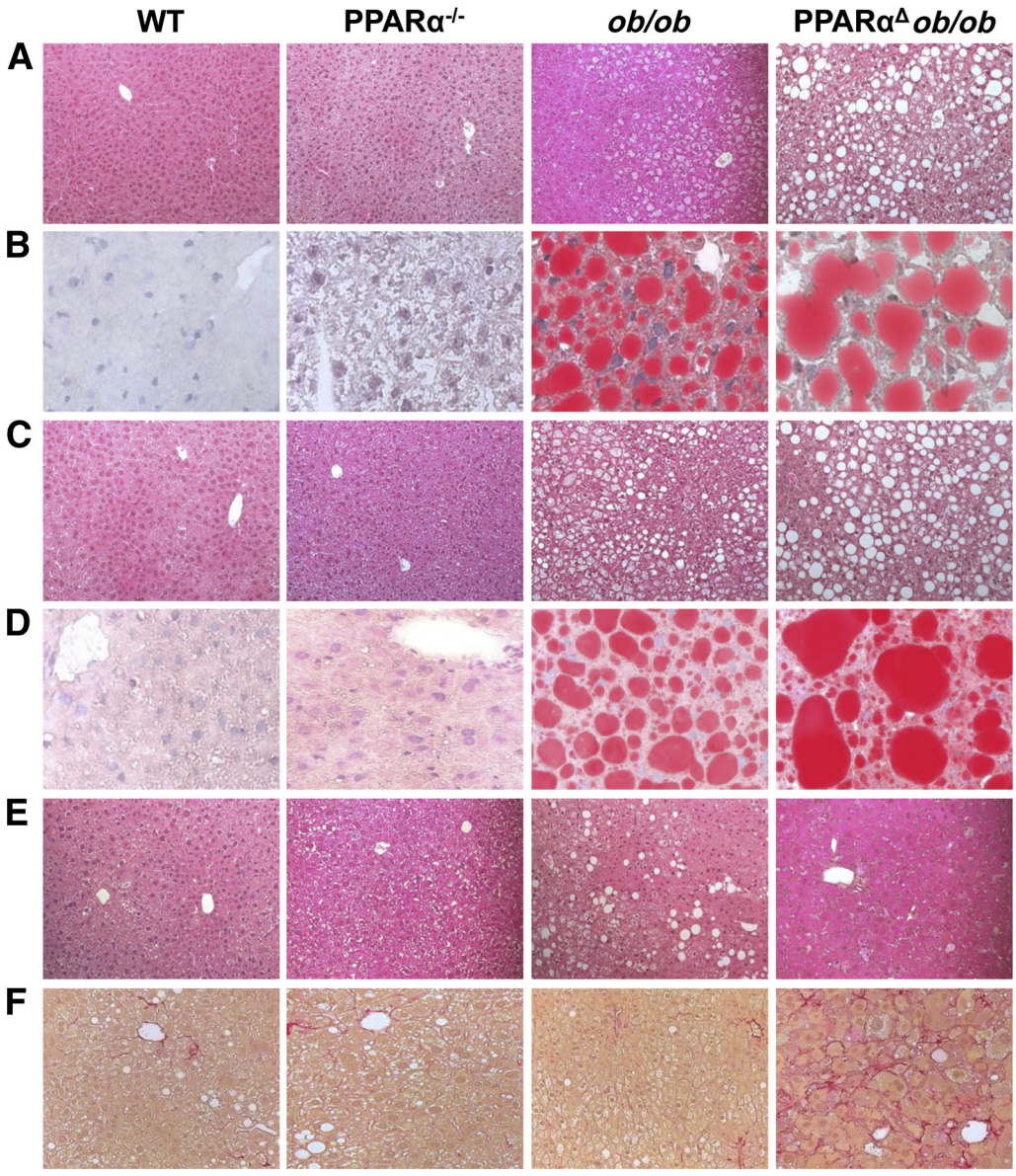

Figure 3 PPARα$^{\Delta}$*ob/ob* mice exhibit severe hepatic steatosis. PPARα deficiency aggravates hepatic steatosis in *ob/ob* mice (see *ob/ob* versus PPARα$^{\Delta}$*ob/ob*). Liver sections of 3-month-old (**A** and **B**), 6-month-old (**C** and **D**), 16-month-old (**E**) wild-type (WT), PPARα$^{-/-}$, *ob/ob*, and PPARα$^{\Delta}$*ob/ob* mice maintained on a chow diet were stained with hematoxylin and eosin (**A**, **C**, and **E**) and Oil Red O (**B** and **D**). **F:** Sirius Red staining of liver sections of 16-month-old mice. PPARα$^{\Delta}$*ob/ob* mice reveal a discernible increase in Sirius Red–positive fibrous septa.

microsomal ω-oxidation pathways to generate ketone bodies that include acetoacetate, 3-hydroxybutyrate (alias β-hydroxybutyrate), and acetone.[38] These serve as fuel for nonhepatic peripheral tissues.[38] Because PPARα is vital for the transcriptional regulation of fatty acid–metabolizing enzymes in liver, the deficiency of this transcription factor in starvation leads to hepatic steatosis.[39,40] To ascertain the combined effects of decreased energy burning due to PPARα deficiency and increased food intake due to lack of leptin during starvation, WT, PPARα$^{-/-}$, *ob/ob*, and PPARα$^{\Delta}$*ob/ob* mice were fasted for 24, 48, and 72 hours (Figure 4). After 24 hours starvation, PPARα$^{-/-}$ and PPARα$^{\Delta}$*ob/ob* mouse livers were paler and larger, suggestive of fatty change when compared to fasted WT and *ob/ob* livers (Figure 4A). The difference in pallor was exaggerated with prolonged fasting (Figure 4A). In contrast, pallor in *ob/ob* mouse liver was reduced after starvation (Figure 4A).

Hematoxylin and eosin and Oil O Red staining results confirmed severe hepatic steatosis in PPARα$^{-/-}$ and PPARα$^{\Delta}$*ob/ob* mice after starvation (Figure 4, B and C). Hepatic steatosis observed in fed *ob/ob* mice diminished due to fasting-induced activation of PPARα regulated fatty acid oxidation in liver (Figure 4, B and C). No fat droplets are seen in WT and *ob/ob* mouse livers starved for 48 and 72 hours (Figure 4, B and C). The glycogen content in livers of all animals was reduced after fasting (data not shown). Serum glucose levels of PPARα$^{-/-}$ and PPARα$^{\Delta}$*ob/ob* mice were reduced to approximately 47% and 30.3% of basal level

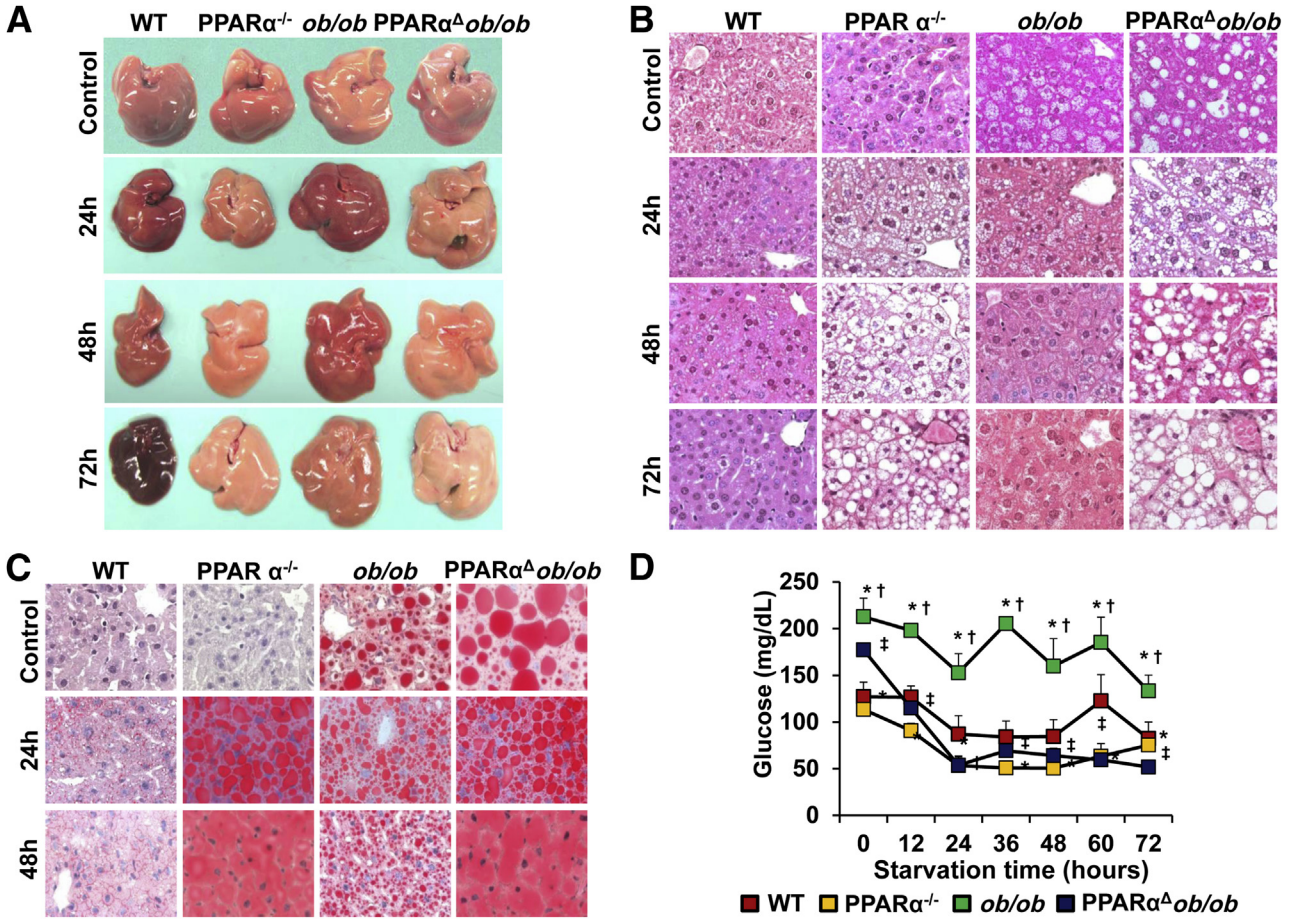

Figure 4 PPARα deficiency increases hepatic steatosis after starvation and reduces plasma glucose significantly. **A:** Representative gross images of livers of fed and 24-, 48-, and 72-hour fasted wild-type (WT), PPARα$^{-/-}$, *ob/ob*, and PPARα$^{\Delta}$*ob/ob* mice. **B:** Hematoxylin and eosin staining of livers of WT, PPARα$^{-/-}$, *ob/ob*, and PPARα$^{\Delta}$*ob/ob* mice fed and fasted for 24, 48, and 72 hours. **C:** Oil Red O—stained liver sections confirm fat accumulation in PPARα$^{-/-}$ and PPARα$^{\Delta}$*ob/ob* mice, but attenuation of steatosis in *ob/ob* mice. **D:** Plasma glucose levels are higher in *ob/ob* mice compared to other genotypes. $^{*}P < 0.05$ versus WT, $^{\dagger}P < 0.05$ versus PPARα$^{-/-}$, and $^{\ddagger}P < 0.05$ versus *ob/ob*.

after 24 hours starvation, respectively, and no further reduction was noted with prolonged fasting (Figure 4D).

Northern and Western blot analyses of liver samples obtained from WT and *ob/ob* mice starved for 24 hours revealed increases in the mRNA and/or protein levels of Acox1, L-PBE (*EHHADH*), MCAD, long-chain acyl-CoA dehydrogenase, CYP4A1, CYP4A3, and fibroblast growth factor 21 after 24 hours of fasting (Figure 5, A and B). Quantitative PCR data revealed increases in PPARα level in livers of fasted WT and *ob/ob* mice (Figure 5). Increased mRNA content of peroxisome proliferator-activated receptor gamma, coactivator 1 alpha (PGC1α) was noted in 24- and 48-hour fasted WT livers. Sirt1 level increased in PPARα$^{\Delta}$*ob/ob* mouse liver at 48 and 72 hours starvation, and phosphoenolpyruvate carboxykinase level increased in normal and *ob/ob* mouse livers at 48 hours of fasting (Figure 5C).

PPARα Ligand Does Not Induce Liver Tumors in PPARα$^{\Delta}$*ob/ob* Mice

Previous studies have shown that increased FAO and energy combustion in liver leads to liver tumor development.[15] Sustained activation of PPARα in *ob/ob* mice attenuates obesity by increasing hepatic FAO but increases the risk for liver tumor development, in part, related to excess energy combustion.[22] To study the influence of PPARα deficiency in PPARα$^{\Delta}$*ob/ob* mice, we first evaluated the effects of short-term administration of Wy-14643, a PPARα ligand (Figure 6). We found, as expected, that PPARα$^{\Delta}$*ob/ob* mice fail to respond to PPARα ligand Wy-14,643 administered in powdered chow at 0.125% for 4 days (Figures 6 and 7).

Induction of PPARα-regulated genes in liver, in particular those involved in FAO, was not observed in PPARα$^{\Delta}$*ob/ob* mice (Figure 6). We also evaluated BrdUrd incorporation in hepatocyte nuclei and expression level of L-PBE, the second enzyme of the peroxisomal β-oxidation, by immunohistochemical analyses (Figure 7, A and B). The liver/body weight ratio increased in WT and *ob/ob* mice fed Wy-14,643 for 4 days, but no increase was evident in PPARα$^{\Delta}$*ob/ob* mice (Figure 7C). BrdUrd labeling indices in liver increased variably in WT and *ob/ob* mice given Wy-14,643 (Figure 7, A and D). It would appear that the increased nuclear labeling in these mice is

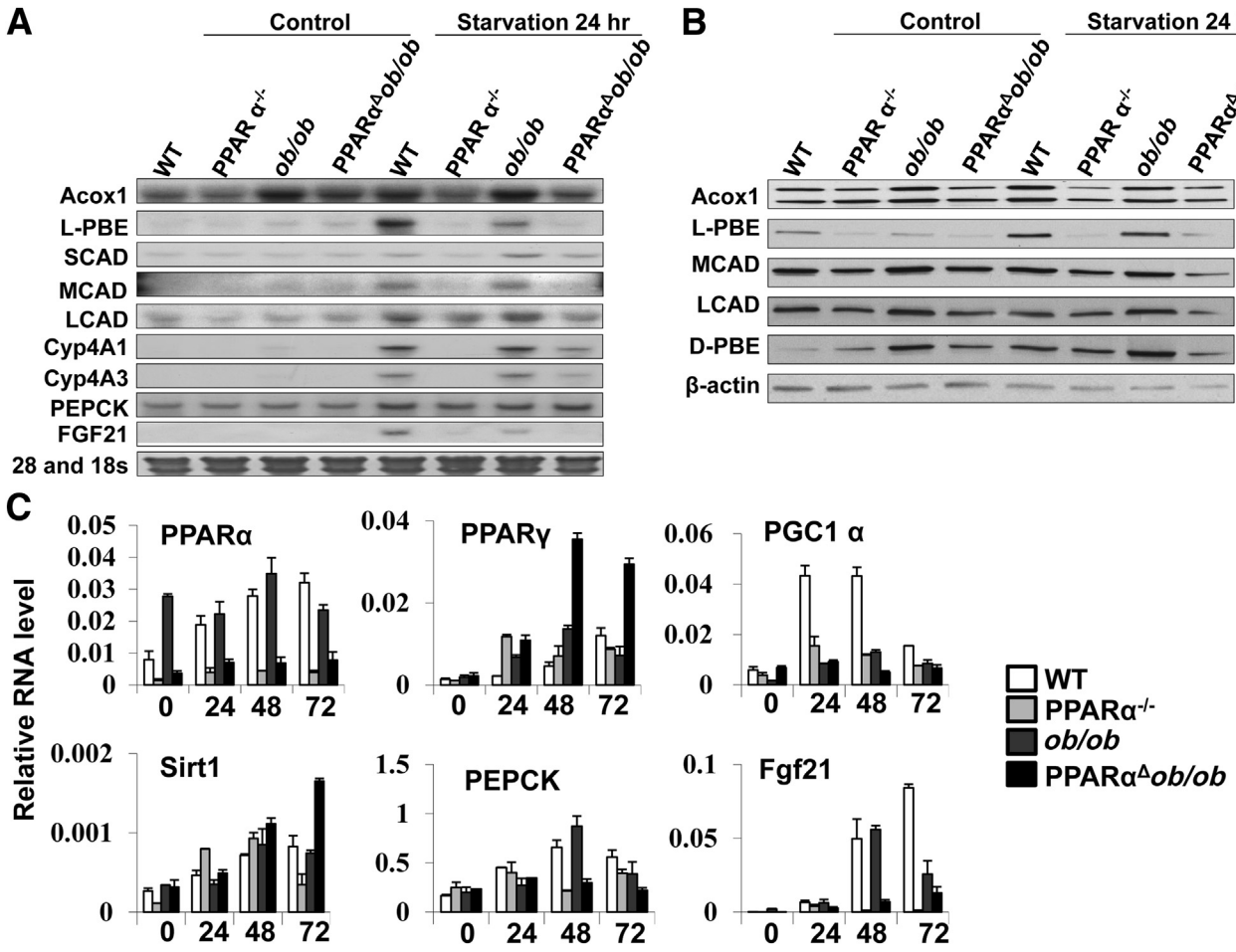

Figure 5 Constitutive and 24-hour starvation inducible levels of fatty acid oxidation gene expression in livers of wild-type (WT), PPARα$^{-/-}$, *ob/ob*, and PPARα$^{\Delta}$*ob/ob* mice. Representative Northern (**A**) and Western (**B**) blots to assess the gene expression changes in liver. **C:** Quantitative PCR data of key enzymes linked to acute fasting. Acox, acyl-Coenzyme A oxidase; D-PBE, D-3-hydroxyacyl-CoA dehydratase; FGF, fibroblast growth factor; LCAD, long-chain acyl-CoA dehydrogenase; L-PBE, L-3-hydroxyacyl-CoA dehydrogenase; MCAD, medium-chain acyl-CoA dehydrogenase; PEPCK, phosphoenolpyruvate carboxykinase; PGC, peroxisome proliferator-activated receptor gamma, coactivator; SCAD, short-chain acyl-CoA dehydrogenase.

PPARα linked, and the small, but perceptible, increase in control and Wy-14,643–treated PPARα$^{\Delta}$*ob/ob* mice is *PPARα* independent.

Sustained activation of PPARα by both synthetic and endogenous ligands results in the development of hepatocellular carcinomas in mice.[15,22,32] Herein, we examined the role of chronic exposure to PPARα ligand Wy-14,643 in PPARα$^{\Delta}$*ob/ob* mice (Figure 8). In WT and *ob/ob* mice chronically fed a Wy-14,643–containing diet, body weights were lower than the chow-fed controls, whereas absence of PPARα, in PPARα$^{-/-}$ mice and PPARα$^{\Delta}$*ob/ob* mice, exerted no significant change in body weights (Figure 8, A and B). All mice that survived were sacrificed at 52 weeks of age, and liver tumor incidence was obtained (Figure 8, C and D). Although all *ob/ob* mice survived at 1 year, the survival probability was reduced during this period in PPARα$^{\Delta}$*ob/ob* mice. Liver tumors were seen in 9 of 10 WT, and 10 of 11 *ob/ob*, mice fed PPARα ligand, but the incidence of liver tumors in *ob/ob* mice maintained on normal chow was low (3/12). PPARα$^{\Delta}$*ob/ob* mice fed a normal or Wy-14,643–containing diet had tumor incidence similar to that of chow-fed *ob/ob* mice. No liver tumors were detected in PPARα$^{-/-}$ mice maintained on a control (0/10) or Wy-14,643–containing diet (0/10). We included data obtained from *Acox1*$^{-/-}$ and Acox1$^{\Delta}$*ob/ob* mice on a control diet. Both these groups with sustained *PPARα* activation due to endogenous ligands developed a high incidence of liver tumors. All tumors were well to moderately differentiated hepatocellular carcinomas.

Discussion

PPARα and Energy Burning

Activation of lipid-sensing nuclear receptor PPARα in liver promotes the uptake, use, and catabolism of fatty acids by transcriptional up-regulation of genes involved in these physiological processes.[8,16,33,41] In liver, PPARα plays a central role in the regulation of energy burning by peroxisomal and mitochondrial fatty acid β-oxidation and microsomal ω-oxidation.[8,15] PPARα is activated by a plethora of synthetic exogenous ligands that include fibrate and other

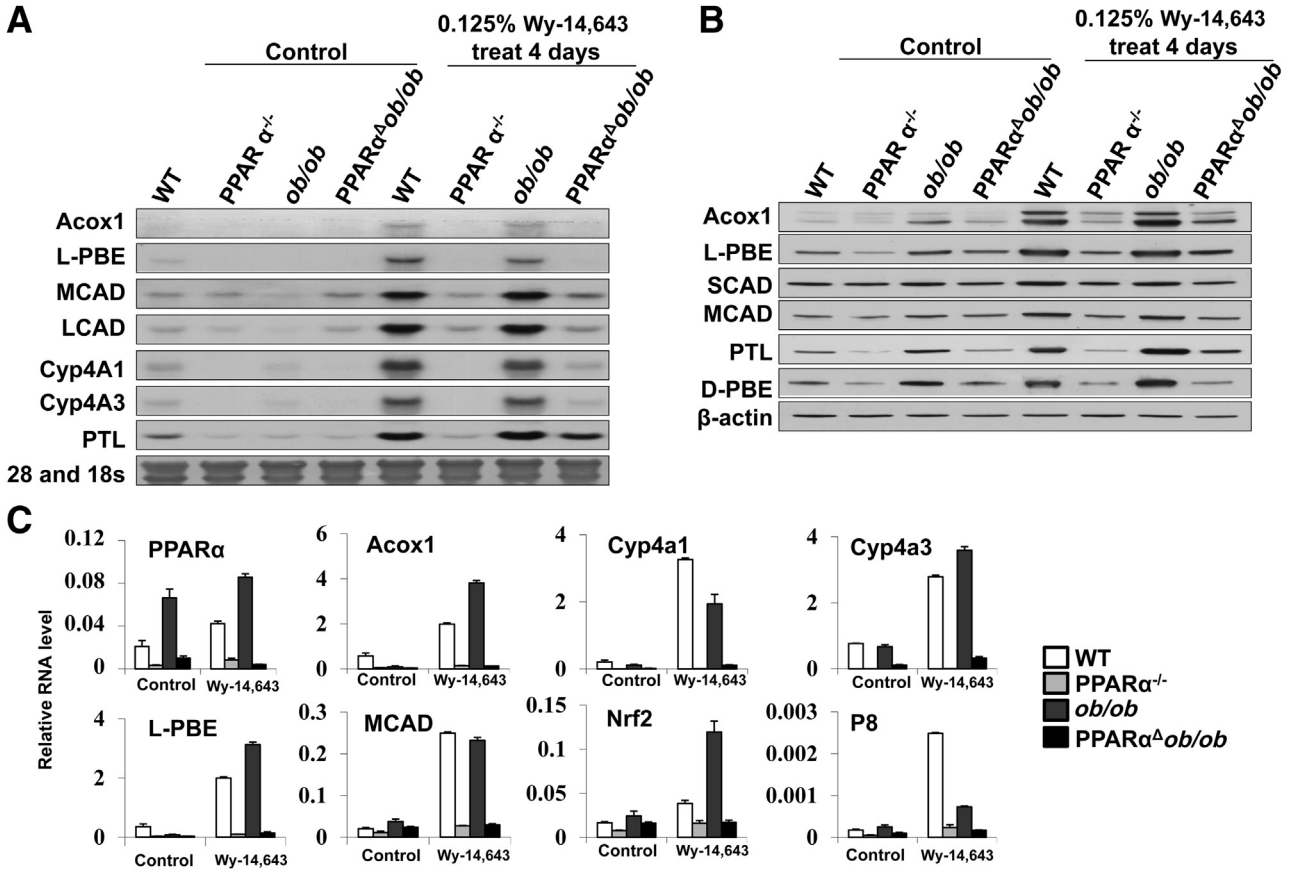

Figure 6 Constitutive and Wy-14,643—inducible levels of fatty acid oxidation gene expression in livers of wild-type (WT), PPARα$^{-/-}$, *ob/ob*, and PPARα$^{\Delta}$*ob/ob* mice. Representative Northern (**A**) and Western (**B**) blots to assess the gene expression changes in liver. **C:** Quantitative PCR data of key enzymes linked to fatty acid oxidation. Acox, acyl-Coenzyme A oxidase; D-PBE, D-3-hydroxyacyl-CoA dehydratase; LCAD, long-chain acyl-CoA dehydrogenase; L-PBE, L-3-hydroxyacyl-CoA dehydrogenase; MCAD, medium-chain acyl-CoA dehydrogenase; PTL, 3-ketoacyl-CoA thiolase; SCAD, short-chain acyl-CoA dehydrogenase.

classes of drugs used in the treatment of hyperlipidemia and also by industrial plasticizers, insecticides, herbicides, and certain organic solvents that are collectively referred to as peroxisome proliferators.[15–17]

Metabolic Pathways that Generate and Degrade Endogenous PPARα Ligands Exist to Modulate Lipid Metabolism: Acox1 in the Metabolism of Endogenous PPARα Activators

The existence of endogenous biological molecules that activate PPARα *in vivo* first became evident in mice with the germline deletion of Acox1, the first and rate-limiting enzyme of the peroxisomal fatty acid β-oxidation pathway.[20,32] Acox1 deficiency results in the generation of a lean mouse with a complex hepatic phenotype manifesting as steatohepatitis, hepatocellular regeneration with massive spontaneous proliferation of peroxisomes, and concomitant perpetually heightened transcriptional activation of PPARα-regulated genes.[20,32] The *Acox1*-null mice also develop a high incidence of hepatocellular carcinomas.[32] These effects are attributed to *Acox1* substrates, such as long-chain and very-long-chain fatty acids, fatty acyl CoAs, and other biological molecules that remain unmetabolized in the absence of Acox1; some of these substrates then function as endogenous activators of PPARα.[32] Thus, Acox1 was the first enzyme demonstrated to be involved in the metabolism of endogenous PPARα ligands.[32] Subsequent studies with other mice with defects in enzymes of FAO established the concept that metabolic pathways that generate and degrade endogenous PPARα ligands exist to modulate lipid metabolism. The sustained overexpression of PPARα-regulated genes involved in FAO in *Acox1*$^{-/-}$ mice contributes to increased energy burning; consequently, these mice develop lean body mass.[20,32]

We have previously reported that Acox1$^{\Delta}$*ob/ob* mice attenuates obesity and hepatic steatosis, along with an increase in insulin sensitivity.[22] As expected, in these Acox1$^{\Delta}$*ob/ob* mice, unmetabolized substrates of Acox1 function as endogenous ligands of PPARα to cause sustained transcriptional activation of PPARα and enhanced FAO.[16,20,32,42] It is, thus, clear that excess energy burning diminishes the development of obesity in *ob/ob* mice, with the genetic model of obesity representing excess energy consumption.[22,35] Activation of *PPARα* in Acox1$^{\Delta}$*ob/ob*

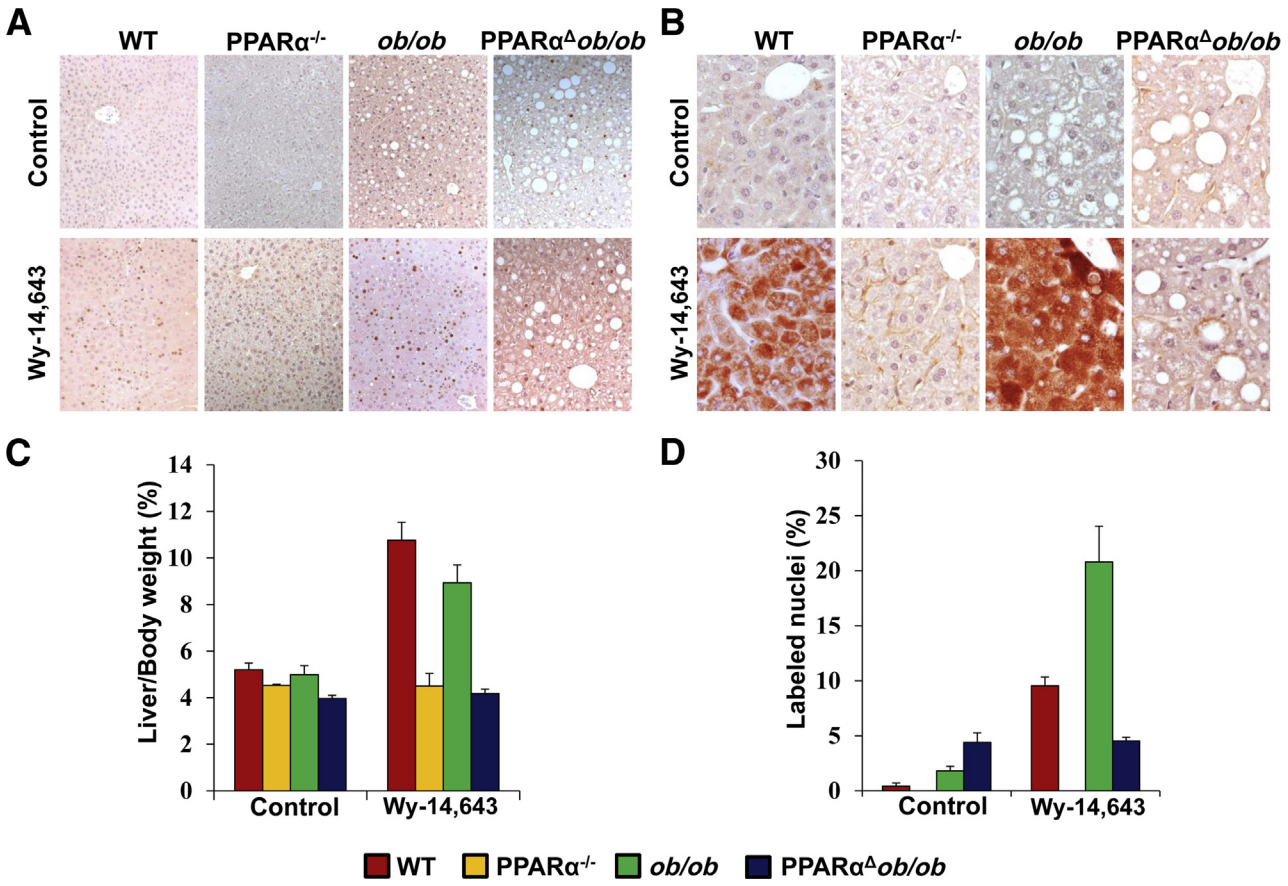

Figure 7 Liver cell proliferation and induction of L-3-hydroxyacyl-CoA dehydrogenase (L-PBE) resulting from PPARα activation by dietary Wy-14,643 for 4 days. Bromodeoxyuridine (BrdUrd) labeling (**A**) and L-PBE immunohistochemical staining (**B**) of livers of 2-month-old wild-type (WT), PPARα$^{-/-}$, *ob/ob*, and PPARα$^{\Delta}$*ob/ob* mice fed with chow diet or 0.125% Wy-14,643 for 4 days. Liver/body weight ratio (**C**) and hepatocyte proliferation (**D**) assessed by BrdUrd labeling ratio by calculating BrdUrd-positive hepatocyte nuclei.

mice increased the expression of genes associated with inflammation and endoplasmic reticulum stress systems contributing to liver tumor development.[22]

Insights from the PPARα$^{\Delta}$*ob/ob* Mice

As a corollary, to establish that the failure to induce PPARα-regulated hepatic fatty acid oxidation and energy burning in *ob/ob* mice impedes the progression of fatty liver disease and development of liver tumors, we generated PPARα$^{\Delta}$*ob/ob* mice. In contrast to Acox1$^{\Delta}$*ob/ob* mice that consumed more energy due to lack of leptin but also burnt excess energy in view of the heightened PPARα-regulated fatty acid oxidation, PPARα$^{\Delta}$*ob/ob* mice, as expected, also consumed more energy due to leptin deficiency but burnt less energy due to PPARα deficiency. PPARα$^{\Delta}$*ob/ob* mice gained more body weight from the age of 24 weeks when compared to *ob/ob* mice, although they consumed less food per gram weight than *ob/ob* mice, suggesting a reduction in energy expenditure associated with PPARα deficiency. The excess energy is conserved in WAT in *ob/ob* and PPARα$^{\Delta}$*ob/ob* mice and accounts for increase in fat weight and adipocyte size.[8–10] As the process progresses, whitening of BAT ensues. Deletion of PPARα in *ob/ob* mice aggravated fat accumulation in adipocytes, resulting in hypertrophic fat cells.

Leptin encoded by *ob* gene regulates appetite, energy homeostasis,[41,43,44] and immune function.[41–45] Its expression level in the adipocytes is correlated with the lipid content and the corresponding individual adipocyte size.[45] Disruption of *ob* gene results in excess food intake with reduced energy expenditure, which accelerates fat accumulation in adipose tissue and liver and influences whitening of BAT.[46–48] As a result, *ob/ob* mice become obese with increased body weight and several fold increase in fat content compared to WT mice, and become hyperinsulinemic and hyperglycemic.[46–48] Because PPARα modulates energy homeostasis, its deletion contributes to the failure to activate fatty acid oxidation systems, which results in an accelerated accumulation of excess energy, first in the adipose tissue and then in the liver. Accordingly, as shown herein, deficiency of PPARα aggravates obesity and hepatic steatosis in *ob/ob* mice and influences insulin and glucose tolerance. In this context, some PPARα ligands have been shown to reduce hyperinsulinemia and hyperglycemia and increase insulin sensitivity of mice fed with a high-fat diet.[46,49] These observations suggest that PPARα deficiency leads to

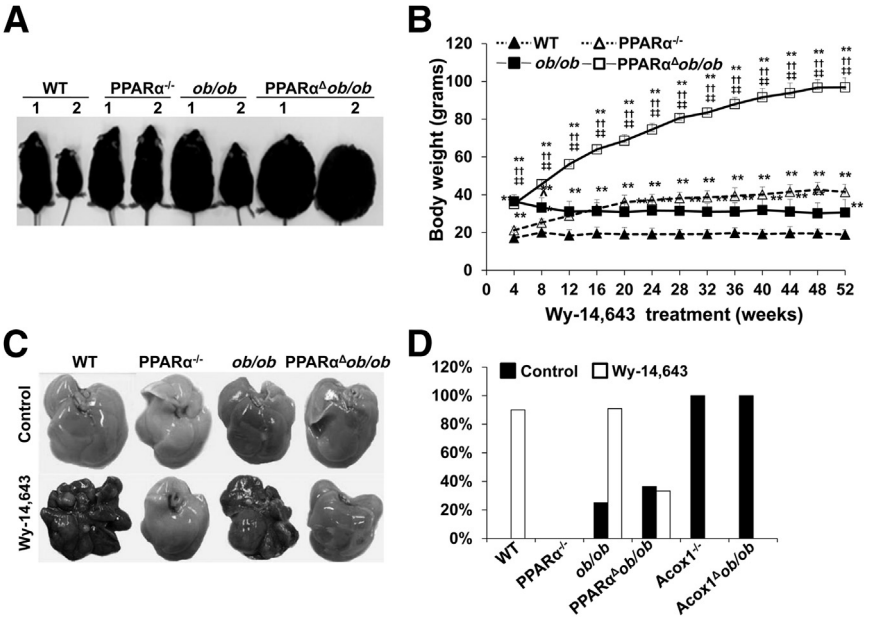

Figure 8 PPARα$^{\Delta}$*ob/ob* mice fail to respond to PPARα ligand Wy-14,643 induced body weight reduction and liver tumorigenesis. **A:** Physical appearance of chow-fed (1) or 0.05% Wy-14,643—fed (2) for 14 months (aged 16 months) wild-type (WT), PPARα$^{-/-}$, *ob/ob*, and PPARα$^{\Delta}$*ob/ob* mice. **B:** Body weight changes of mice treated with 0.05% Wy-14,643 for 8 to 52 weeks. **C:** Liver appearance of WT, PPARα$^{-/-}$, *ob/ob*, and PPARα$^{\Delta}$*ob/ob* mice fed normal chow (control) or treated with 0.05% Wy-14,643 for 14 months. Liver tumors are seen in Wy-14,643—fed WT and *ob/ob* mice. **D:** Incidence of liver tumors. PPARα activation by Wy-14,643 induces liver tumors in *ob/ob* mice, but absence of PPARα in *ob/ob* mice attenuates liver tumorigenesis. All *Acox1*-null mice and Acox1$^{\Delta}$*ob/ob* mice develop liver tumors because of sustained PPARα activation by endogenous ligands. $^{**}P < 0.01$ versus WT, $^{\dagger\dagger}P < 0.01$ versus PPARα$^{-/-}$, and $^{\ddagger\ddagger}P < 0.01$ versus *ob/ob*.

impaired fatty acid oxidation, which aggravates fat accumulation and influences metabolic syndrome in *ob/ob* mice. In this regard, adenoviral-mediated hyperleptinemia induces PPARα transcription and activation of its target genes and reduces hepatic triacylglycerol content.[47] Because adenoviral-mediated induction is transient, the effects of hyperleptinemia reversed as the expression level of PPARα decreased, and fat was regained 2 months after the level of leptin return to normal.[47,48,50,51] Moreover, PPARα expression can be programmed by neonatal leptin administration in rat, which reverses the phenotypic effects of maternal undernutrition.[52,53] Leptin can induce liver-specific promoter activity via a STAT3/Sp1 mechanism.[54] These data suggest that leptin deficiency in PPARα$^{-/-}$ mice attenuates PPARα activity, to further reduce FAO.

Interestingly, aging attenuated hepatic steatosis in both *ob/ob* mice and PPARα$^{\Delta}$*ob/ob* mice. Small cells with oval nuclei arose in both the periphery of the portal tracts and within the hepatic lobular part in PPARα$^{\Delta}$*ob/ob* mouse livers. These cells stained positively for hepatic oval cell markers A6, CD45, CK19, and epithelial cell adhesion molecule. Similar cells were not evident in the livers of WT, PPARα$^{-/-}$, and *ob/ob* mice. Hepatic oval cells, regarded as stem/progenitor cells in adult livers, can be activated under Dipin, partial hepatectomy, and chronic liver injury conditions.[55–59] After chronic injury or impaired proliferation of hepatocytes, facultative adult oval cells proliferate and differentiate into hepatocytes and epithelial cells. Chemical hepatotoxic substances and continuous metabolic stress can thus be considered as potential oval cell activators. In the livers of PPARα$^{\Delta}$*ob/ob* mice, severe hepatic steatosis, because of excess fat overload and damaged FAO, leads to hepatocyte apoptosis, with new hepatocyte proliferation independent of PPARα to replace the dead cells.

During acute fasting, metabolic substrates are switched from carbohydrate to fatty acids, which leads to the release of large quantities of free fatty acids from adipose tissue into circulation, reaching the liver. In the liver, fatty acids are metabolized to generate ketone bodies to serve as fuels for other tissues. In WT and *ob/ob* mice, the intact PPARα senses the influx of fatty acids resulting from starvation to up-regulate enzymes involved in FAO.[39,40] We noted a marked increase in Cyp4a1 and Cyp4a3 mRNA levels. During fasting, PGC1α, Sirt1, and fibroblast growth factor 21 were also induced in WT and *ob/ob* mice. Fasting stimulated an increase in fatty acid mobilization, and an increase in FAO resulted in the reduction of hepatic steatosis in *ob/ob* mice, which have intact PPARα. Deletion of PPARα in *ob/ob* mice resulted in severe hepatic steatosis and reduction in plasma glucose level after 24 hours of starvation. FAO enzymes were not induced because of PPARα deficiency. In PPARα-deleted *ob/ob* mice, PPARγ and Sirt1 expression was induced after starvation, but the relevance is unclear. Furthermore, PPARα$^{-/-}$ mice and PPARα$^{\Delta}$*ob/ob* mice fail to respond to Wy-14,643, a potent synthetic PPARα activator. In the absence of PPARα, there is no induction of fatty acid oxidation, peroxisome proliferation, and liver tumorigenesis in PPARα$^{-/-}$ mice and PPARα$^{\Delta}$*ob/ob* mice. Previous work has shown that fat accumulation in the livers of *ob/ob* mice alone will not lead to liver tumors, but sustained activation of PPARα-modulated energy expenditure by endogenous PPARα ligands in *ob/ob* mice resulted in liver tumor development.[22] On the other hand, PPARα deficiency in *ob/ob* mice further aggravates hepatic steatosis, but does not increase the liver tumor risk, suggesting that fat accumulation in liver is not the direct reason for hepatocellular carcinoma.

In summary, these observations further support the notion that PPARα-regulated signaling plays an important role in

the progression of liver diseases in obese mice. PPARα deficiency aggravates obesity-associated hepatic steatosis without increasing liver cancer risk in *ob/ob* mice, whereas heightened activation of PPARα in *ob/ob* fatty livers increases the risk of liver cancer.

Supplemental Data

Supplemental material for this article can be found at *http://dx.doi.org/10.1016/j.ajpath.2015.01.018*.

References

1. Ng M, Fleming T, Robinson M, Thomson B, Graetz N, Margono C, et al: Global, regional, and national prevalence of overweight and obesity in children and adults during 1980-2013: a systematic analysis for the Global Burden of Disease Study 2013. Lancet 2014, 384: 766−781
2. Nguyen BT, Powell LM: The impact of restaurant consumption among US adults: effects on energy and nutrient intakes. Public Health Nutr 2014, 17:2445−2452
3. Reddy JK: Nonalcoholic steatosis and steatohepatitis, III: peroxisomal beta-oxidation, PPAR alpha, and steatohepatitis. Am J Physiol Gastrointest Liver Physiol 2001, 281:G1333−G1339
4. Reddy JK, Rao MS: Lipid metabolism and liver inflammation, II: fatty liver disease and fatty acid oxidation. Am J Physiol Gastrointest Liver Physiol 2006, 290:G852−G858
5. Park EJ, Lee JH, Yu GY, He G, Ali SR, Holzer RG, Osterreicher CH, Takahashi H, Karin M: Dietary and genetic obesity promote liver inflammation and tumorigenesis by enhancing IL-6 and TNF expression. Cell 2010, 140:197−208
6. Cohen JC, Horton JD, Hobbs HH: Human fatty liver disease: old questions and new insights. Science 2011, 332:1519−1523
7. Agopian VG, Kaldas FM, Hong JC, Whittaker M, Holt C, Rana A, Zarrinpar A, Petrowsky H, Farmer D, Yersiz H, Xia V, Hiatt JR, Busuttil RW: Liver transplantation for nonalcoholic steatohepatitis: the new epidemic. Ann Surg 2012, 256:624−633
8. Evans RM, Barish GD, Wang YX: PPARs and the complex journey to obesity. Nat Med 2004, 10:355−361
9. Liu L, Mei M, Yang S, Li Q: Roles of chronic low-grade inflammation in the development of ectopic fat deposition. Mediators Inflamm 2014, 2014:418185
10. Gurevich-Panigrahi T, Panigrahi S, Wiechec E, Los M: Obesity: pathophysiology and clinical management. Curr Med Chem 2009, 16: 506−521
11. Tacke F, Luedde T, Trautwein C: Inflammatory pathways in liver homeostasis and liver injury. Clin Rev Allergy Immunol 2009, 36: 4−12
12. Fabbrini E, Sullivan S, Klein S: Obesity and nonalcoholic fatty liver disease: biochemical, metabolic, and clinical implications. Hepatology 2010, 51:679−689
13. Faggioni R, Jones-Carson J, Reed DA, Dinarello CA, Feingold KR, Grunfeld C, Fantuzzi G: Leptin-deficient (ob/ob) mice are protected from T cell-mediated hepatotoxicity: role of tumor necrosis factor alpha and IL-18. Proc Natl Acad Sci U S A 2000, 97:2367−2372
14. Huang J, Viswakarma N, Yu S, Jia Y, Bai L, Vluggens A, Cherkaoui-Malki M, Khan M, Singh I, Yang G, Rao MS, Borensztajn J, Reddy JK: Progressive endoplasmic reticulum stress contributes to hepatocarcinogenesis in fatty acyl-CoA oxidase 1-deficient mice. Am J Pathol 2011, 179:703−713
15. Misra P, Reddy JK: Peroxisome proliferator-activated receptor-alpha activation and excess energy burning in hepatocarcinogenesis. Biochimie 2014, 98:63−74
16. Pyper SR, Viswakarma N, Yu S, Reddy JK: PPARalpha: energy combustion, hypolipidemia, inflammation and cancer. Nucl Recept Signal 2010, 8:e002
17. Gonzalez FJ, Shah YM: PPARalpha: mechanism of species differences and hepatocarcinogenesis of peroxisome proliferators. Toxicology 2008, 246:2−8
18. Hays T, Rusyn I, Burns AM, Kennett MJ, Ward JM, Gonzalez FJ, Peters JM: Role of peroxisome proliferator-activated receptor-alpha (PPARalpha) in bezafibrate-induced hepatocarcinogenesis and cholestasis. Carcinogenesis 2005, 26:219−227
19. Palkar PS, Anderson CR, Ferry CH, Gonzalez FJ, Peters JM: Effect of prenatal peroxisome proliferator-activated receptor alpha (PPARalpha) agonism on postnatal development. Toxicology 2010, 276:79−84
20. Fan CY, Pan J, Chu R, Lee D, Kluckman KD, Usuda N, Singh I, Yeldandi AV, Rao MS, Maeda N, Reddy JK: Hepatocellular and hepatic peroxisomal alterations in mice with a disrupted peroxisomal fatty acyl-coenzyme A oxidase gene. J Biol Chem 1996, 271: 24698−24710
21. Lee SS, Pineau T, Drago J, Lee EJ, Owens JW, Kroetz DL, Fernandez-Salguero PM, Westphal H, Gonzalez FJ: Targeted disruption of the alpha isoform of the peroxisome proliferator-activated receptor gene in mice results in abolishment of the pleiotropic effects of peroxisome proliferators. Mol Cell Biol 1995, 15:3012−3022
22. Huang J, Jia Y, Fu T, Viswakarma N, Bai L, Rao MS, Zhu Y, Borensztajn J, Reddy JK: Sustained activation of PPARalpha by endogenous ligands increases hepatic fatty acid oxidation and prevents obesity in ob/ob mice. FASEB J 2012, 26:628−638
23. Lalloyer F, Vandewalle B, Percevault F, Torpier G, Kerr-Conte J, Oosterveer M, Paumelle R, Fruchart JC, Kuipers F, Pattou F, Fievet C, Staels B: Peroxisome proliferator-activated receptor alpha improves pancreatic adaptation to insulin resistance in obese mice and reduces lipotoxicity in human islets. Diabetes 2006, 55:1605−1613
24. Zhou Y, Zhang X, Chen L, Wu J, Dang H, Wei M, Fan Y, Zhang Y, Zhu Y, Wang N, Breyer MD, Guan Y: Expression profiling of hepatic genes associated with lipid metabolism in nephrotic rats. Am J Physiol Renal Physiol 2008, 295:F662−F671
25. Fu T, Mukhopadhyay D, Davidson NO, Borensztajn J: The peroxisome proliferator-activated receptor alpha (PPARalpha) agonist ciprofibrate inhibits apolipoprotein B mRNA editing in low density lipoprotein receptor-deficient mice: effects on plasma lipoproteins and the development of atherosclerotic lesions. J Biol Chem 2004, 279: 28662−28669
26. Fu T, Borensztajn J: Simvastatin causes the formation of cholesterol-rich remnants in mice lacking apoE. Biochem Biophys Res Commun 2006, 341:1172−1176
27. Bai L, Jia Y, Viswakarma N, Huang J, Vluggens A, Wolins NE, Jafari N, Rao MS, Borensztajn J, Yang G, Reddy JK: Transcription coactivator mediator subunit MED1 is required for the development of fatty liver in the mouse. Hepatology 2011, 53:1164−1174
28. Miura K, Yang L, van Rooijen N, Brenner DA, Ohnishi H, Seki E: Toll-like receptor 2 and palmitic acid cooperatively contribute to the development of nonalcoholic steatohepatitis through inflammasome activation in mice. Hepatology 2013, 57:577−589
29. Jia Y, Qi C, Kashireddi P, Surapureddi S, Zhu YJ, Rao MS, Le Roith D, Chambon P, Gonzalez FJ, Reddy JK: Transcription coactivator PBP, the peroxisome proliferator-activated receptor (PPAR)-binding protein, is required for PPARalpha-regulated gene expression in liver. J Biol Chem 2004, 279:24427−24434
30. Viswakarma N, Jia Y, Bai L, Gao Q, Lin B, Zhang X, Misra P, Rana A, Jain S, Gonzalez FJ, Zhu YJ, Thimmapaya B, Reddy JK: The Med1 subunit of the mediator complex induces liver cell proliferation and is phosphorylated by AMP kinase. J Biol Chem 2013, 288:27898−27911
31. Yu S, Matsusue K, Kashireddy P, Cao WQ, Yeldandi V, Yeldandi AV, Rao MS, Gonzalez FJ, Reddy JK: Adipocyte-specific gene expression and adipogenic steatosis in the mouse liver due to peroxisome proliferator-activated receptor gamma1 (PPARgamma1) overexpression. J Biol Chem 2003, 278:498−505

32. Fan CY, Pan J, Usuda N, Yeldandi AV, Rao MS, Reddy JK: Steatohepatitis, spontaneous peroxisome proliferation and liver tumors in mice lacking peroxisomal fatty acyl-CoA oxidase: implications for peroxisome proliferator-activated receptor alpha natural ligand metabolism. J Biol Chem 1998, 273:15639–15645
33. Issemann I, Green S: Activation of a member of the steroid hormone receptor superfamily by peroxisome proliferators. Nature 1990, 347: 645–650
34. Reddy JK, Goel SK, Nemali MR, Carrino JJ, Laffler TG, Reddy MK, Sperbeck SJ, Osumi T, Hashimoto T, Lalwani ND, Rao MS: Transcription regulation of peroxisomal fatty acyl-CoA oxidase and enoyl-CoA hydratase/3-hydroxyacyl-CoA dehydrogenase in rat liver by peroxisome proliferators. Proc Natl Acad Sci U S A 1986, 83:1747–1751
35. Halaas JL, Gajiwala KS, Maffei M, Cohen SL, Chait BT, Rabinowitz D, Lallone RL, Burley SK, Friedman JM: Weight-reducing effects of the plasma protein encoded by the obese gene. Science 1995, 269:543–546
36. Nikoozad Z, Ghorbanian MT, Rezaei A: Comparison of the liver function and hepatic specific genes expression in cultured mesenchymal stem cells and hepatocytes. Iran J Basic Med Sci 2014, 17:27–33
37. Petersen BE, Goff JP, Greenberger JS, Michalopoulos GK: Hepatic oval cells express the hematopoietic stem cell marker Thy-1 in the rat. Hepatology 1998, 27:433–445
38. van den Berghe G: The role of the liver in metabolic homeostasis: implications for inborn errors of metabolism. J Inherit Metab Dis 1991, 14:407–420
39. Kersten S, Seydoux J, Peters JM, Gonzalez FJ, Desvergne B, Wahli W: Peroxisome proliferator-activated receptor alpha mediates the adaptive response to fasting. J Clin Invest 1999, 103:1489–1498
40. Hashimoto T, Cook WS, Qi C, Yeldandi AV, Reddy JK, Rao MS: Defect in peroxisome proliferator-activated receptor alpha-inducible fatty acid oxidation determines the severity of hepatic steatosis in response to fasting. J Biol Chem 2000, 275:28918–28928
41. Park HK, Ahima RS: Leptin signaling. F1000Prime Rep 2014, 6:73
42. Reddy JK, Hashimoto T: Peroxisomal beta-oxidation and peroxisome proliferator-activated receptor alpha: an adaptive metabolic system. Annu Rev Nutr 2001, 21:193–230
43. Zhou YT, Shimabukuro M, Koyama K, Lee Y, Wang MY, Trieu F, Newgard CB, Unger RH: Induction by leptin of uncoupling protein-2 and enzymes of fatty acid oxidation. Proc Natl Acad Sci U S A 1997, 94:6386–6390
44. Shimabukuro M, Koyama K, Chen G, Wang MY, Trieu F, Lee Y, Newgard CB, Unger RH: Direct antidiabetic effect of leptin through triglyceride depletion of tissues. Proc Natl Acad Sci U S A 1997, 94: 4637–4641
45. Maffei M, Fei H, Lee GH, Dani C, Leroy P, Zhang Y, Proenca R, Negrel R, Ailhaud G, Friedman JM: Increased expression in adipocytes of ob RNA in mice with lesions of the hypothalamus and with mutations at the db locus. Proc Natl Acad Sci U S A 1995, 92:6957–6960
46. Guerre-Millo M, Gervois P, Raspe E, Madsen L, Poulain P, Derudas B, Herbert JM, Winegar DA, Willson TM, Fruchart JC, Berge RK, Staels B: Peroxisome proliferator-activated receptor alpha activators improve insulin sensitivity and reduce adiposity. J Biol Chem 2000, 275:16638–16642
47. Lee Y, Yu X, Gonzales F, Mangelsdorf DJ, Wang MY, Richardson C, Witters LA, Unger RH: PPAR alpha is necessary for the lipopenic action of hyperleptinemia on white adipose and liver tissue. Proc Natl Acad Sci U S A 2002, 99:11848–11853
48. Orci L, Cook WS, Ravazzola M, Wang MY, Park BH, Montesano R, Unger RH: Rapid transformation of white adipocytes into fat-oxidizing machines. Proc Natl Acad Sci U S A 2004, 101:2058–2063
49. Ye JM, Doyle PJ, Iglesias MA, Watson DG, Cooney GJ, Kraegen EW: Peroxisome proliferator-activated receptor (PPAR)-alpha activation lowers muscle lipids and improves insulin sensitivity in high fat-fed rats: comparison with PPAR-gamma activation. Diabetes 2001, 50:411–417
50. Wang MY, Lee Y, Unger RH: Novel form of lipolysis induced by leptin. J Biol Chem 1999, 274:17541–17544
51. Zhou YT, Wang ZW, Higa M, Newgard CB, Unger RH: Reversing adipocyte differentiation: implications for treatment of obesity. Proc Natl Acad Sci U S A 1999, 96:2391–2395
52. Gluckman PD, Lillycrop KA, Vickers MH, Pleasants AB, Phillips ES, Beedle AS, Burdge GC, Hanson MA: Metabolic plasticity during mammalian development is directionally dependent on early nutritional status. Proc Natl Acad Sci U S A 2007, 104: 12796–12800
53. Vickers MH, Gluckman PD, Coveny AH, Hofman PL, Cutfield WS, Gertler A, Breier BH, Harris M: Neonatal leptin treatment reverses developmental programming. Endocrinology 2005, 146:4211–4216
54. Garratt ES, Vickers MH, Gluckman PD, Hanson MA, Burdge GC, Lillycrop KA: Tissue-specific 5' heterogeneity of PPARalpha transcripts and their differential regulation by leptin. PLoS One 2013, 8: e67483
55. Fox IJ, Roy-Chowdhury J: Hepatocyte transplantation. J Hepatol 2004, 40:878–886
56. Jochheim-Richter A, Rudrich U, Koczan D, Hillemann T, Tewes S, Petry M, Kispert A, Sharma AD, Attaran F, Manns MP, Ott M: Gene expression analysis identifies novel genes participating in early murine liver development and adult liver regeneration. Differentiation 2006, 74:167–173
57. Golding M, Sarraf CE, Lalani EN, Anilkumar TV, Edwards RJ, Nagy P, Thorgeirsson SS, Alison MR: Oval cell differentiation into hepatocytes in the acetylaminofluorene-treated regenerating rat liver. Hepatology 1995, 22:1243–1253
58. Petersen BE, Zajac VF, Michalopoulos GK: Hepatic oval cell activation in response to injury following chemically induced periportal or pericentral damage in rats. Hepatology 1998, 27:1030–1038
59. Davies RA, Knight B, Tian YW, Yeoh GC, Olynyk JK: Hepatic oval cell response to the choline-deficient, ethionine supplemented model of murine liver injury is attenuated by the administration of a cyclo-oxygenase 2 inhibitor. Carcinogenesis 2006, 27:1607–1616